Synthesis and Characterization of Chitosan-Based Polystyrene composite and Evaluation of its Optical Properties

Prashant D. Yeram[1], Sandip B. Ghodile[2*] and Pradeep Jain[3]
[1]Research Scholar, Department of Chemistry, Janata Mahavidyalaya, Chandrapur, Maharashtra, India
[2]Assistant Professor, Department of Chemistry, Mahatma Gandhi College of Science, Gadchandur, Maharashtra, India
[3]Assistant Professor, Department of Chemistry, C. L. Jain (P.G.) College, Firozabad

***Corresponding Author:** sandipghodile2@gmail.com

ABSTRACT
The development of biodegradable polymer composites with improved physicochemical properties has become an important research focus for sustainable advanced materials. In this study, a chitosan–polystyrene (CS–PS) composite was synthesized through solution blending followed by glutaraldehyde-mediated chemical crosslinking. The structural, morphological, elemental and optical characteristics of the synthesized material were systematically investigated using Fourier Transform Infrared (FTIR) spectroscopy, X-ray Diffraction (XRD), Scanning Electron Microscopy (SEM), Energy Dispersive X-ray Spectroscopy (EDS), solid-state ^{13}C CP/MAS Nuclear Magnetic Resonance (NMR) spectroscopy and UV–Visible spectroscopy. FTIR and solid-state ^{13}C NMR analyses confirmed the successful incorporation of polystyrene within the chitosan matrix through the coexistence of characteristic functional groups and carbon environments. XRD patterns exhibited a broad diffraction peak centered at approximately 18.7° SEM micrographs revealed a compact and heterogeneous morphology while EDS spectra verified carbon, nitrogen and oxygen as the principal elemental constituents of the composite. UV–Visible spectroscopy demonstrated strong ultraviolet absorption with a maximum absorption wavelength of approximately 269 nm indicating enhanced optical performance. The synergistic combination of chitosan and polystyrene produced a composite with improved structural integrity and favorable optical characteristics suggesting its suitability for advanced applications in optical materials, protective coatings, sustainable packaging and multifunctional polymer-based systems.
Keywords: Chitosan, Optical Properties, Polystyrene, Polymer Composite, Physical Properties
How to cite this article: Yeram PD, Ghodile SB, Jain P. Synthesis and Characterization of Chitosan-Based Polystyrene composite and Evaluation of its Optical Properties. Int J Drug Deliv Technol. 2026;16(69s): 307-313. DOI: 10.25258/ijddt.16.69s.32

1. INTRODUCTION

The growing need for sustainable materials with improved functional performance has led to increasing interest in biopolymer-based composites. Among the available biopolymers, chitosan has emerged as a promising material because of its biodegradability, biocompatibility, non-toxicity, antimicrobial properties and excellent film-forming ability [1]. Despite these advantages its practical application is often limited by poor mechanical strength, high moisture sensitivity and moderate thermal stability [2]. Blending chitosan with suitable synthetic polymers has therefore become an effective strategy for overcoming these limitations and improving its overall performance [3]. Polystyrene is a widely used thermoplastic polymer valued for its optical transparency, dimensional stability, low density, and ease of processing. Combining chitosan with polystyrene offers an opportunity to integrate the environmental benefits of a natural polymer with the desirable optical and mechanical properties of a synthetic polymer [4]. The interactions between these two polymers can significantly influence the structural and functional characteristics of the resulting composite, making it suitable for a range of advanced material applications [5]. The optical performance of polymer composites is closely related to their molecular structure and morphology. Parameters such as absorbance, transmittance, absorption coefficient, extinction coefficient, optical band gap and Urbach energy provide important information about their electronic structure and optical behavior [6]. However systematic studies that correlate the structural, optical and physical properties of chitosan–polystyrene composites remain limited [7]. In this work a chitosan-based polystyrene composite was synthesized and comprehensively characterized to investigate its structural, optical and physical properties. The results are expected to improve the understanding of structure–property relationships in these composites and support their potential use in advanced optical, electronic, and functional polymer applications.

2. Materials and Methods

2.1 Materials

Chitosan (CS) derived from shrimp shells (molecular weight: 3,800–20,000 g mol^{-1}; degree of deacetylation ≥75%) and polystyrene (PS) were

purchased from HiMedia Laboratories Pvt. Ltd., India. Chitosan was used as the natural polymer matrix whereas polystyrene served as the synthetic polymer component. A 25% aqueous glutaraldehyde solution was employed as the crosslinking agent. Glacial acetic acid was used to dissolve chitosan while N,N-dimethylformamide (DMF) was used as the solvent for polystyrene. All reagents were of analytical grade and used without further purification.

2.2 Methods

2.2.1 Preparation of Chitosan–Polystyrene Composite

The CS–PS composite film was prepared by a solution-casting method. Initially 2 g of chitosan was dissolved in 100 mL of 2% aqueous acetic acid under magnetic stirring for 4 h to obtain a homogeneous solution. Thereafter 15 mL of 25% glutaraldehyde was added slowly with continuous stirring to promote crosslinking within the chitosan matrix. Separately, 2 g of polystyrene was dissolved in 50 mL of DMF until a clear solution was obtained [8]. The polystyrene solution was then added gradually to the crosslinked chitosan solution and stirred for an additional 4 h to ensure uniform mixing. The resulting blend was cast into a polystyrene Petri dish and dried in a hot-air oven at 40–50 °C until complete solvent evaporation. The dried composite film was removed carefully and stored in a desiccator prior to optical and physical characterization [9].

2.2.2 Optical Properties Measurement

The optical characteristics of the synthesized chitosan–polystyrene (CS–PS) copolymer were evaluated using ultraviolet–visible (UV–Vis) spectroscopy. Spectral measurements were performed with a Shimadzu UV–VIS–IR spectrophotometer (Model: UV-3600 Plus) across the wavelength range of 200–800 nm under ambient laboratory conditions. The prepared copolymer specimens were analyzed to investigate their optical absorption behavior and the associated electronic transitions occurring within the ultraviolet and visible spectral regions. The recorded absorption spectra provided valuable information regarding the interaction of electromagnetic radiation with the copolymer matrix. Furthermore the spectral features were interpreted to examine the effect of copolymerization on the electronic structure and optical response of the synthesized material [10].

2.2.3 Characterization Techniques

The structural, chemical and morphological characteristics of the synthesized chitosan–polystyrene (CS–PS) copolymer were comprehensively investigated using multiple analytical techniques. Solid-state 13C nuclear magnetic resonance (NMR) spectroscopy was employed to examine the carbon framework and elucidate the molecular interactions between the chitosan backbone and polystyrene segments [11]. Fourier transform infrared (FTIR) spectroscopy was utilized to identify the characteristic functional groups and to verify the successful formation of the copolymer through chemical bonding analysis. X-ray diffraction (XRD) analysis was performed to evaluate changes in crystallinity and structural organization induced by the copolymerization process [12]. In addition, the surface morphology and elemental composition of the synthesized material were examined using scanning electron microscopy (SEM) coupled with energy-dispersive X-ray spectroscopy (EDS) providing detailed insights into its microstructural features and elemental distribution.

3. RESULTS AND DISCUSSION

3.1 FTIR ANALYSIS

FT-IR spectroscopy was performed to investigate the chemical structure of the synthesized chitosan–polystyrene (CS–PS) composite and to confirm the molecular interactions developed during glutaraldehyde-assisted crosslinking. The FT-IR spectrum (Figure 1) exhibits the characteristic absorption bands of both chitosan and polystyrene demonstrating the successful formation of the composite. A broad absorption band at 3428.50 cm^{-1} is assigned to the overlapping O–H and N–H stretching vibrations of chitosan. The broadness of this peak indicates extensive hydrogen bonding within the composite matrix, suggesting strong intermolecular interactions between chitosan and polystyrene [13]. The absorption bands at 3075.92 cm^{-1} and 2928.61 cm^{-1} correspond to aromatic and aliphatic C–H stretching vibrations respectively, confirming the successful incorporation of polystyrene into the chitosan matrix. The weak bands observed at 1948.86 cm^{-1} and 1875.04 cm^{-1} are attributed to aromatic combination and overtone vibrations which are characteristic of the benzene ring in polystyrene [14]. A distinct absorption band at 1650.40 cm^{-1} is assigned to C=N and amide-related stretching vibrations. This band confirms the formation of Schiff-base (imine) linkages through the reaction of glutaraldehyde with the amino groups of chitosan providing clear evidence of successful chemical crosslinking. The peaks at 1444.68 cm^{-1} and 1379.75 cm^{-1} correspond to CH_2 bending and aromatic skeletal vibrations respectively, further confirming the presence of the polystyrene phase in the composite. The absorption band at 1048.44 cm^{-1} is attributed to C–O stretching of the chitosan polysaccharide backbone indicating that the structural integrity of chitosan was retained during composite formation. The fingerprint region exhibits characteristic polystyrene bands at 757.35 cm^{-1} and 693.71 cm^{-1} assigned to aromatic C–H out-of-plane bending and monosubstituted benzene ring vibrations respectively [15]. The FT-IR results confirm the successful synthesis of the CS–PS composite

through glutaraldehyde-mediated crosslinking. The coexistence of characteristic absorption bands of chitosan and polystyrene, together with the appearance of the C=N stretching band, demonstrates effective chemical integration of the two polymers. The combined effects of covalent crosslinking and hydrogen bonding are expected to enhance the structural stability and functional properties of the composite.

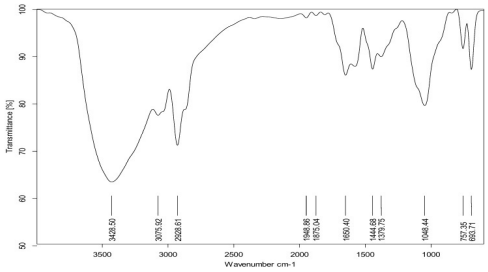

Figure 1. FTIR spectrum of chitosan–polystyrene (CS–PS) composite.

3.2 XRD ANALYSIS

The structural characteristics of the synthesized chitosan-based polystyrene (CS–PS) composite were investigated by X-ray diffraction (XRD) and the corresponding diffraction pattern is shown in Figure 2. The diffraction profile exhibits a broad and intense peak centered at approximately 2θ = 18.7° along with a weak shoulder around 11–13°. No sharp crystalline reflections were observed throughout the scanned range (5–80°) indicating that the synthesized composite possesses a predominantly amorphous structure with limited long-range molecular ordering [17]. The continuous decrease in diffraction intensity beyond 25° without the appearance of additional diffraction peaks further confirms the absence of crystalline phases and demonstrates the homogeneous dispersion of polystyrene within the chitosan matrix. The broad diffraction halo is characteristic of amorphous polymeric materials and indicates successful molecular integration of the constituent polymers. Therefore, the XRD results confirm the successful formation of a chemically crosslinked chitosan–polystyrene composite with a homogeneous amorphous microstructure, which is expected to contribute positively to its optical and physical properties [18].

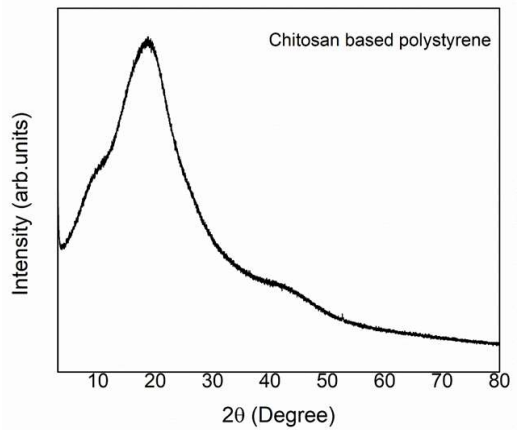

Figure 2. XRD pattern of chitosan–polystyrene (CS–PS) composite

3.3 SEM ANALYSIS

The surface morphology of the synthesized chitosan–polystyrene (CS–PS) composite was investigated using scanning electron microscopy (SEM), and the representative micrographs are presented in Figure 3 (a–l). The SEM images revealed that blending chitosan with polystyrene followed by glutaraldehyde crosslinking produced a compact and interconnected polymeric structure with heterogeneous surface features [19]. At lower magnifications (Figure 3 (a–b)), the composite exhibited irregular folded domains and a rough surface, indicating the formation of a three-dimensional polymer network. Higher-magnification images (Fig. 3 (c–h)) showed a dense and continuous matrix with localized roughness and uniformly distributed particulate features. The absence of distinct phase-separated regions or large voids suggests good compatibility and strong interfacial adhesion between chitosan and polystyrene, confirming the successful incorporation of polystyrene within the chitosan matrix [20]. The micrographs in Fig. 3 (i–l) revealed a few localized surface microcracks with widths ranging from approximately 2.7 to 3.2 μm, which are attributed to film shrinkage during solvent evaporation and drying. However, these cracks remained isolated and did not disrupt the continuity of the polymer matrix, indicating that the crosslinked structure effectively resisted extensive crack propagation. The SEM observations confirm the successful synthesis of a homogeneous and structurally stable CS–PS composite. The compact morphology, interconnected polymer network, and limited microcracking are expected to enhance the composite's physical stability and influence its optical performance, making the material suitable for advanced functional polymer applications.

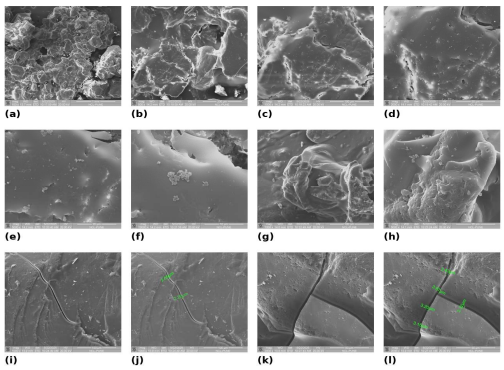

Figure 3. SEM micrographs of the synthesized chitosan–polystyrene (CS–PS) composite recorded at different magnifications and selected regions: **(a–l)** representative surface morphologies illustrating the microstructural characteristics of the composite.

3.4 EDS ANALYSIS

Energy-dispersive X-ray spectroscopy (EDS) was performed to investigate the elemental composition of the synthesized chitosan–polystyrene (CS–PS) composite and to verify the successful integration of both polymeric constituents. The corresponding EDS spectrum (Figure 4) exhibits distinct signals associated exclusively with carbon (C), nitrogen (N) and oxygen (O) confirming that the composite consists predominantly of the expected elemental constituents without detectable contamination from foreign elements. Carbon was identified as the predominant element with a weight percentage of 66.10 wt.%, followed by oxygen at 26.82 wt.% and nitrogen at 7.07 wt.% [21]. The oxygen content is attributed mainly to the abundant hydroxyl groups present in the chitosan matrix, whereas the nitrogen signal originates from the primary amino functionalities characteristic of chitosan. The elemental distribution obtained from EDS is consistent with the expected chemical composition of the CS–PS composite [22]. Moreover the absence of additional elemental peaks demonstrates that no significant inorganic impurities or residual precursor species remained after synthesis, indicating the effectiveness of the preparation process. The observed elemental composition provides direct evidence for the successful formation of the chitosan–polystyrene composite and complements the structural information obtained from FTIR and XRD analyses thereby confirming the integrity of the synthesized material.

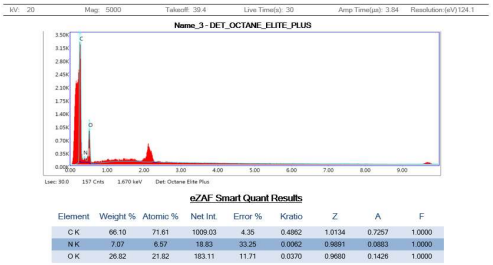

Figure 4. EDS spectrum of the synthesized chitosan–polystyrene (CS–PS) composite

3.5 UV–VISIBLE SPECTROSCOPY AND OPTICAL PROPERTIES

The UV–Visible absorption spectrum of the synthesized chitosan–polystyrene (CS–PS) composite was recorded over the wavelength range of 200–800 nm as shown in Figure 5. The spectrum exhibits a strong absorption band in the ultraviolet region with a maximum at approximately 269 nm followed by a gradual decrease in absorbance toward the visible region (800 nm). This behavior indicates efficient absorption of high-energy UV photons and comparatively low absorption in the visible region [23]. The absorption peak at 269 nm is attributed to π–π^* electronic transitions of the aromatic phenyl rings present in polystyrene. The incorporation of polystyrene introduces aromatic chromophores into the chitosan matrix resulting in enhanced ultraviolet absorption compared with pristine chitosan. The enhanced UV absorption confirms the successful incorporation of polystyrene within the chitosan network and demonstrates modification of the composite's electronic structure. The UV–Visible analysis verifies the formation of a homogeneous composite with improved optical performance suitable for advanced optical and protective applications [24].

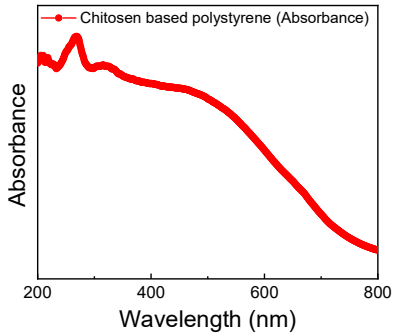

Figure 5. UV–Visible absorption spectrum of the chitosan–polystyrene (CS–PS) composite

3.6 Solid-State ^{13}C CP/MAS NMR Analysis

The solid-state ^{13}C CP/MAS NMR spectrum of the synthesized chitosan–polystyrene (CS–PS) composite **(**Figure 6**)** confirms the presence of characteristic carbon environments from both chitosan and polystyrene indicating successful

composite formation. A prominent resonance at 128.27 ppm is assigned to the aromatic carbon atoms of the polystyrene phenyl rings. The signals at 146.64 and 145.28 ppm are attributed to substituted aromatic carbons influenced by intermolecular interactions within the composite [25]. The resonance at 100.68 ppm corresponds to the anomeric carbon (**C1**) of chitosan, while the peaks at 76.20 and 60.91 ppm are assigned to the oxygenated carbon atoms (**C3–C6**) of the chitosan backbone, confirming that its primary structure is retained after composite formation. The resonances at 45.84, 40.81, 37.33, 32.06 and 26.76 ppm are attributed to aliphatic carbon environments associated with the crosslinked polymer network formed through interactions among chitosan, polystyrene, and glutaraldehyde [26]. The coexistence of aromatic and polysaccharide carbon signals demonstrates effective incorporation of polystyrene into the chitosan matrix. The NMR results are consistent with the FTIR and XRD analyses confirming successful synthesis of the CS–PS composite.

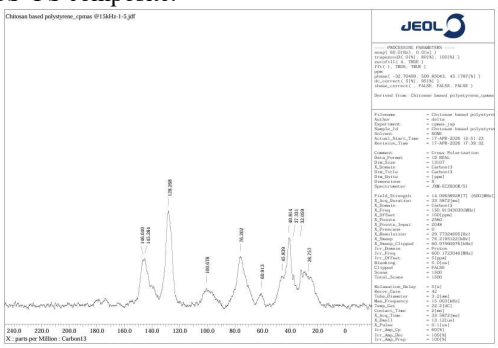

Figure 6. Solid-state ^{13}C CP/MAS NMR spectrum of the synthesized chitosan–polystyrene (CS–PS) composite

3.7 Evaluation of Optical Properties

The optical properties of the synthesized chitosan-based polystyrene (CS–PS) copolymer were investigated using UV–Visible spectroscopy over the wavelength range of 200–800 nm. The absorption spectrum revealed strong absorption in the ultraviolet region with the maximum absorbance (2.883) observed at 269 nm, followed by a gradual decrease towards the visible region, reaching 0.344 at 800 nm. This behaviour is attributed to the $\pi \rightarrow \pi^*$ transitions of the aromatic rings of polystyrene and the $n \rightarrow \pi^*$ transitions associated with the oxygen-containing functional groups of chitosan [27]. The corresponding transmittance increased progressively from 0.27% at 200 nm to 45.29% at 800 nm indicating excellent UV-blocking capability and moderate transparency in the visible region. The absorption coefficient (α) calculated using the Beer–Lambert relation was highest in the ultraviolet region and gradually decreased with increasing wavelength confirming efficient photon absorption at higher energies. Similarly the extinction coefficient (k) exhibited low values throughout the investigated spectral range, indicating minimal optical losses within the polymer matrix. The optical band gap (Eg= 3.1) was estimated from the Tauc plot (Figure 7). The obtained optical parameters confirm that the synthesized CS–PS copolymer behaves as a wide-band-gap polymeric material with good optical transparency, low optical attenuation and promising potential for UV-protective coatings, transparent films and optoelectronic applications (Table 1) [28].

Table 1. Optical Parameters of Chitosan-Based Polystyrene Copolymer

Wavelength (nm)	Absorbance (A)	Transmittance (%)	Absorption Coefficient, α (cm^{-1})	Extinction Coefficient, k
200	2.566	0.27	1181.90	0.00188
250	2.697	0.20	1242.24	0.00247
300	2.509	0.31	1155.65	0.00276
400	2.323	0.48	1069.97	0.00341
500	2.142	0.72	986.61	0.00393
600	1.531	2.94	705.18	0.00337
700	0.769	17.02	354.20	0.00197
800	0.344	45.29	158.45	0.00101

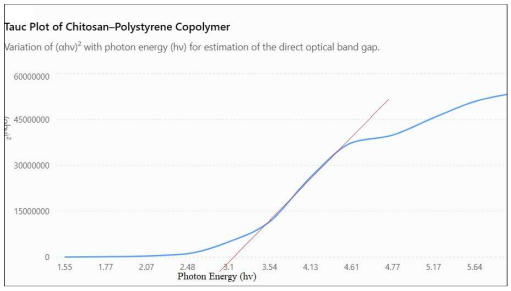

Figure 7. Tauc Plot of Chitosan-Polystyrene Composite

4. CONCLUSION

A chitosan–polystyrene (CS–PS) composite was successfully synthesized through solution blending followed by glutaraldehyde crosslinking. FTIR, XRD, SEM, EDS and solid-state ^{13}C CP/MAS NMR analyses collectively confirmed the successful incorporation of polystyrene into the chitosan matrix. The composite exhibited a predominantly amorphous structure with a broad XRD peak at approximately 18.7°, a compact and heterogeneous surface morphology and the expected elemental composition of carbon,

nitrogen and oxygen. UV–Visible analysis revealed strong absorption in the ultraviolet region with a maximum absorption near 269 nm indicating favorable optical characteristics. The agreement between the NMR, FTIR and XRD results further verified the structural integrity of the synthesized composite. These findings demonstrate that the CS–PS composite possesses improved optical and physical properties making it a promising material for optical devices, protective coatings, packaging and other advanced polymer-based applications. Further studies involving DSC, TGA, mechanical, dielectric and application-specific performance evaluations will provide a more comprehensive understanding of the composite and support its potential for practical technological applications.

Acknowledgements:

The author sincerely acknowledges the Sophisticated Analytical Instrument Facility (SAIF), IIT Bombay, for providing the Nuclear Magnetic Resonance (NMR) spectrometer facility and support for obtaining characterization data of the Chitosan-based Polystyrene (CS–PS) sample used in this research work. The author also gratefully acknowledges CSIR–National Chemical Laboratory (NCL), Pune, for providing instrumental facilities and support for obtaining characterization data of the Chitosan-based Polystyrene (CS–PS) samples used in this study through Fourier Transform Infrared Spectroscopy (FTIR), Scanning Electron Microscopy coupled with Energy Dispersive X-ray Spectroscopy (SEM–EDS), UV–Visible spectroscopy, and X-ray Diffraction (XRD) analyses.

References

1. Lehocký, M. (2025). Environmental Applications of Chitosan Derivatives and Chitosan Composites. *Polymers*, *17*(19), 2583. https://doi.org/10.3390/polym17192583
2. Sabo, Dini & Habibu, Shehu & Ladan, Magaji & Abdullahi, Shuaibu & Eric, Daniel. (2025). Development of Starch-based Biodegradable Plastics reinforced with Natural Fiber for enhanced mechanical and biodegradation properties. UMYU Scientifica. 4. 338-358. 10.56919/usci.2544.030.
3. Kaur, M., Sharma, A., Puri, V., Aggarwal, G., Maman, P., Huanbutta, K., Nagpal, M., & Sangnim, T. (2023). Chitosan-Based Polymer Blends for Drug Delivery Systems. *Polymers*, *15*(9), 2028. https://doi.org/10.3390/polym15092028
4. Okolie, O., Kumar, A., Edwards, C., Lawton, L. A., Oke, A., McDonald, S., Thakur, V. K., & Njuguna, J. (2023). Bio-Based Sustainable Polymers and Materials: From Processing to Biodegradation. *Journal of Composites Science*, *7*(6), 213. https://doi.org/10.3390/jcs7060213
5. Oladele, Isiaka & Onuh, Nnabuike Linus & Siengchin, Suchart & M R, Sanjay & Adelani, Samson. (2023). Modern Applications of Polymer Composites in Structural Industries: A Review of Philosophies, Product Development, and Graphical Applications. Applied Science and Engineering Progress. 6884. 10.14416/j.asep.2023.07.003.
6. Aziz, S. B., Nofal, M. M., Brza, M. A., Hussein, S. A., Mahmoud, K. H., El-Bahy, Z. M., Dannoun, E. M. A., Kareem, W. O., & Hussein, A. M. (2021). Characteristics of PEO Incorporated with $CaTiO_3$ Nanoparticles: Structural and Optical Properties. *Polymers*, *13*(20), 3484. https://doi.org/10.3390/polym13203484
7. Zhuikova, Y., Zhuikov, V., & Varlamov, V. (2022). Biocomposite Materials Based on Poly(3-hydroxybutyrate) and Chitosan: A Review. *Polymers*, *14*(24), 5549. https://doi.org/10.3390/polym14245549
8. Pelayo-Vázquez, J. B., Osuna-Laveaga, D. R., Peña-Jaramillo, J. P., Gómez-Salazar, S., Moreno-Medrano, E. D., & Pérez-García, M. G. (2026). Iron Oxide–Chitosan Macroporous Nanocomposite Hydrogels for Efficient Heterogeneous Electro-Fenton Degradation of Ciprofloxacin. *Gels*, *12*(5), 434. https://doi.org/10.3390/gels12050434
9. Grzybek, P., Jakubski, Ł., & Dudek, G. (2022). Neat Chitosan Porous Materials: A Review of Preparation, Structure Characterization and Application. *International Journal of Molecular Sciences*, *23*(17), 9932. https://doi.org/10.3390/ijms23179932
10. Vega-Hernández, M. Á., Cano-Díaz, G. S., Vivaldo-Lima, E., Rosas-Aburto, A., Hernández-Luna, M. G., Martinez, A., Palacios-Alquisira, J., Mohammadi, Y., & Penlidis, A. (2021). A Review on the Synthesis, Characterization, and Modeling of Polymer Grafting. *Processes*, *9*(2), 375. https://doi.org/10.3390/pr9020375
11. Gartner, Carmiña & Lopez, Betty & Sierra, Ligia & Graf, Robert & Spiess, Hans & Gaborieau, Marianne. (2011). Interplay between Structure and Dynamics in Chitosan Films Investigated with Solid-State NMR, Dynamic Mechanical Analysis, and X-ray Diffraction. Biomacromolecules. 12. 1380–1386. 10.1021/bm200193u.
12. Pasieczna-Patkowska, S., Cichy, M., & Flieger, J. (2025). Application of Fourier

Transform Infrared (FTIR) Spectroscopy in Characterization of Green Synthesized Nanoparticles. *Molecules*, *30*(3), 684. https://doi.org/10.3390/molecules30030684He, Xuemei & Xu, Huidong & Li, Hui. (2015). Cr(VI) Removal from Aqueous Solution by Chitosan/Carboxylmethyl Cellulose/Silica Hybrid Membrane. World Journal of Engineering and Technology. 03. 234-240. 10.4236/wjet.2015.33C034.

13. He, Xuemei & Xu, Huidong & Li, Hui. (2015). Cr(VI) Removal from Aqueous Solution by Chitosan/Carboxylmethyl Cellulose/Silica Hybrid Membrane. World Journal of Engineering and Technology. 03. 234-240. 10.4236/wjet.2015.33C034.
14. Mascarenhas, N. & Gonsalves, R. & Goveas, Jenice & Shekhara, Chandra & Crasta, Vincent. (2016). Preparation and characterization of chitosan - polystyrene polymer blends. 1731. 140039. 10.1063/1.4948205.
15. Al-Kadhemy, Mahasin & Abaas, Wafaa & F. Al-Sharuee, Israa. (2013). The Effect of Gamma Radiation on the FTIR Spectrum of Crystal Violet Doped Polystyrene Films.
16. Hoffmann, B & Seitz, Daniel & Mencke, A & Kokott, A & Ziegler, G. (2009). Glutaraldehyde and oxidised dextran as crosslinker reagents for chitosan-based scaffolds for cartilage tissue engineering. Journal of materials science. Materials in medicine. 20. 1495-503. 10.1007/s10856-009-3707-3.
17. Maniukiewicz, Waldemar. (2010). X-Ray Diffraction Studies of Chitin, Chitosan and Their Derivatives. 10.1201/EBK1439816035-c8.
18. Moreau, Liane & Ha, Don-Hyung & Zhang, Haitao & Hovden, Robert & Muller, David & Robinson, Richard. (2013). Defining Crystalline/Amorphous Phases of Nanoparticles through X-ray Absorption Spectroscopy and X-ray Diffraction: The Case of Nickel Phosphide. Chemistry of Materials. 25. 2394-2403. 10.1021/cm303490y.
19. Mallakpour, Shadpour & Khadem, Elham. (2018). Chitosan/CaCO 3 -silane nanocomposites: Synthesis, characterization, in vitro bioactivity and Cu(II) adsorption properties. International Journal of Biological Macromolecules. 114. 10.1016/j.ijbiomac.2018.03.076.
20. Greenhalgh, Emile. (2009). Failure Analysis and Fractography of Polymer Composites. Failure Analysis and Fractography of Polymer Composites. 1-595.
21. Son, D., Cho, S., Nam, J., Lee, H., & Kim, M. (2020). X-ray-Based Spectroscopic Techniques for Characterization of Polymer Nanocomposite Materials at a Molecular Level. *Polymers*, *12*(5), 1053. https://doi.org/10.3390/polym12051053
22. Akdaşçi, E., Duman, H., Eker, F., Bechelany, M., & Karav, S. (2025). Chitosan and Its Nanoparticles: A Multifaceted Approach to Antibacterial Applications. *Nanomaterials*, *15*(2), 126. https://doi.org/10.3390/nano15020126
23. Aziz, S. B., Brza, M. A., Nofal, M. M., Abdulwahid, R. T., Hussen, S. A., Hussein, A. M., & Karim, W. O. (2020). A Comprehensive Review on Optical Properties of Polymer Electrolytes and Composites. *Materials*, *13*(17), 3675. https://doi.org/10.3390/ma13173675
24. Kaymaz, Sümeyra & Malekzad, Hediyeh & Sarigül, Hasan & Soylukan, Caner & Akyüz, Lalehan & Yüce, Meral. (2023). Nanomaterial surface modification toolkit: Principles, components, recipes, and applications. Advances in Colloid and Interface Science. 322. 103035. 10.1016/j.cis.2023.103035.
25. Younes, Islem & Hajji, Sawssen & Frachet, Véronique & Rinaudo, Marguerite & Jellouli, Kemel & Hajji, V & Frachet, M & Rinaudo, K & Jellouli, M & Nasri, Rim. (2014). Chitin extraction from shrimp shell using enzymatic treatment. Antitumor, antioxidant and antimicrobial activities of chitosan.
26. Silva, Suse & Kaisler, Malgorzata & Broek, Lambertus & Frissen, August & Boeriu, Carmen. (2018). Water-soluble chitosan derivatives and pH-responsive hydrogels by selective C-6 oxidation mediated by TEMPO-laccase redox system. Carbohydrate Polymers. 186. 299-309. 10.1016/j.carbpol.2018.01.050.
27. Recek, N., Primc, G., Vesel, A., Mozetic, M., Avila, J., Razado-Colambo, I., & Asensio, M. C. (2016). Degradation of Albumin on Plasma-Treated Polystyrene by Soft X-ray Exposure. *Polymers*, *8*(7), 244. https://doi.org/10.3390/polym8070244
28. Irbe, Ilze & Spigulis, Janis. (2021). Beer–Lambert law for optical tissue diagnostics: current state of the art and the main limitations. Journal of Biomedical Optics. 26. 100901-100901. 10.1117/1.JBO.26.10.100901.